

## Order parameter in complex dipolar structures: Microscopic modeling

S. Prosandeev<sup>1,2</sup> and L. Bellaiche<sup>1</sup>

<sup>1</sup>Physics Department, University of Arkansas, Fayetteville, Arkansas 72701, USA

<sup>2</sup>Research Institute of Physics, Southern Federal University, 344090 Rostov on Don, Russia

(Received 13 November 2007; revised manuscript received 24 December 2007; published 7 February 2008)

Microscopic models have been used to reveal the existence of an order parameter that is associated with many complex dipolar structures in magnets and ferroelectrics. This order parameter involves a double cross product of the local dipoles with their positions. It provides a measure of subtle microscopic features, such as the helicity of the two domains inherent to onion states, curvature of the dipolar pattern in flower states, or characteristics of sets of vortices with opposite chirality (e.g., distance between the vortex centers and/or the magnitude of their local dipoles).

DOI: [10.1103/PhysRevB.77.060101](https://doi.org/10.1103/PhysRevB.77.060101)

PACS number(s): 77.80.Bh, 75.10.-b, 75.60.Ch, 77.80.Dj

Nanostructures made of dipolar systems have been intensively studied during the last decade, due to the need for miniaturizing devices as well as to the quest for novel phenomena. As a result, many complex dipolar structures have recently been found. Examples include periodic stripe structures and bubbles in thin films made of ferromagnetics or ferroelectrics (see Refs. 1–4 and references therein). Other examples include the so-called onion states, flower states, vortex states, and phases possessing vortices of different chirality in zero-dimensional magnets and/or ferroelectrics (see Refs. 1 and 5–8 and references therein). The high complexity inherent to such dipolar structures can imply that magnetization or polarization is not an order parameter (or at least is not the sole order parameter) associated with their formation and evolution. For instance, one needs to introduce an original quantity, denoted as the toroidal moment, that involves the cross product of the local dipoles with their positions, to describe magnetic or electric vortex states.<sup>6,9,10</sup> In light of such recent findings, it is legitimate to ask if an additional order parameter needs to be defined to fully represent some of the recently discovered complex dipolar structures. Such an additional order parameter, if it indeed exists, is of obvious fundamental and technological importance. As a matter of fact, its existence would imply that general (phenomenological) models would have to be developed in the near future to reproduce and understand the properties of some complex dipolar systems. Similarly, finding a way to control such a hypothetical order parameter may open the door for the design of new devices with original and/or enhanced abilities.

The aim of this present paper is to reveal, via the use of computational schemes, that a specific order parameter has indeed been overlooked. In fact, it is found to characterize many complex dipolar structures, which makes it even more interesting.

Here, we first investigate a ferromagnetic ring that has a height  $h \approx 250$  nm, and internal and external radii about the  $z$  axis (which lies along [001]) equal to  $r \approx 417$  nm and  $L \approx 1056$  nm, respectively. We make this ring asymmetric in shape by shifting along the  $x$  axis (which lies along [100]) the center of the internal circle in any (001) plane from the center of the external circle by  $S \approx 167$  nm. Since the use of fully atomistic techniques to simulate such sizes (which are needed to obtain complex dipolar configurations<sup>5,11,12</sup>) is not currently feasible, we use here the hybrid approach of Ref.

12, which combines both atomistic and continuum features. Technically, the simulated system is divided into equal regions (cells) of volume  $b^3$ , with  $b \approx 83$  nm. The total magnetic moment of any such cell  $j$ ,  $\boldsymbol{\mu}_j$ , is equal to the sum of the  $\mathbf{m}_{i,j}$  local magnetic moments of the magnetic atoms  $i$  belonging to that cell  $j$ , with the assumption that the  $\mathbf{m}_{i,j}$  are all identical inside a given cell  $j$ .<sup>13</sup> The total energy of this ferromagnetic ring under an ac magnetic field,  $\mu_0 \mathbf{H}$  (with  $\mu_0$  being the permeability of vacuum), is given by

$$E_{\text{magn}} = \frac{1}{2} \sum_{j,k,\alpha,\beta} D_{j\alpha,k\beta} \mu_{j\alpha} \mu_{k\beta} - \mu_0 \mathbf{H} \cdot \sum_j \boldsymbol{\mu}_j + \frac{1}{2} J \sum_{j,k\alpha} \mu_{j\alpha} \mu_{k\alpha} \quad (1)$$

where the sums run over the cells  $j$  and  $k$  and over the Cartesian components  $\alpha$  and  $\beta$ . Note that  $D_{j\alpha,k\beta}$  is the tensor associated with the long-range magnetic dipole-dipole interactions,<sup>12</sup> and that the sum over  $k$  in the last term only runs over the first nearest neighbors of the cells  $j$ . The short-range exchange interaction parameter between the  $\boldsymbol{\mu}_j$ 's is estimated from the usual material exchange constant  $A$  as  $J = Aa/(n^5 |\mathbf{m}_{i,j}|^2)$ , where  $a$  is the material primitive lattice constant and where  $n = b/a$  is an integer. We chose a magnetic field of 0.6 MHz frequency applied along the  $y$  axis. This ring is mimicked as being made of Permalloy 80 (i.e.,  $\text{Ni}_{80}\text{Fe}_{20}$ ) by using the parameters<sup>11</sup>  $A = 1.3 \times 10^{-6}$  erg/cm,  $|\mathbf{m}_{i,j}| = 0.205 \mu_B$  (where  $\mu_B$  is the Bohr magneton), and  $a \approx 3$  Å.  $E_{\text{magn}}$  is then used to solve the Landau-Lifshitz molecular dynamics equations<sup>14</sup> for all the  $\boldsymbol{\mu}_j$ .

We also consider ferroelectric nanodots made of  $\text{Pb}(\text{Zr}_{0.4}\text{Ti}_{0.6})\text{O}_3$  (PZT), and having {001} Pb-O terminated surfaces. They are represented by supercells that are finite in any direction, with their total energy being

$$E_{\text{tot}} = E_{\text{mat}}(\{\mathbf{p}_i\}, \{\mathbf{v}_i\}, \hat{\boldsymbol{\eta}}, \{\sigma_i\}) + \frac{1}{2} \beta \sum_i \langle \mathbf{E}_{\text{dep}} \rangle \cdot \mathbf{p}_i + E_{\text{surf}}(\{\mathbf{p}_i\}, \{\mathbf{v}_i\}), \quad (2)$$

where  $\mathbf{p}_i$  is the electrical dipole moment at the site  $i$  of the supercell and  $\mathbf{v}_i$  is a dimensionless vector related to the inhomogeneous strain around this site,<sup>15</sup> while  $\hat{\boldsymbol{\eta}}$  is the homogeneous strain tensor.  $\{\sigma_i\}$  characterizes the alloy configuration,<sup>16</sup> which is presently randomly chosen, in order to mimic a disordered system. The expression and first-

principles-derived parameters of  $E_{\text{mat}}$ , the intrinsic alloy effective Hamiltonian energy, are those given in Ref. 16 for PZT bulk, except for the dipole-dipole interactions, for which we use the analytical expressions derived in Refs. 7 and 17 for our supercells under ideal open-circuit (OC) conditions. Such electrical boundary conditions naturally lead to the existence of a maximum depolarizing field (denoted by  $\langle \mathbf{E}_{\text{dep}} \rangle$  and determined from the atomistic approach of Ref. 7) inside the system for a nonvanishing polarization. The second term of Eq. (2) mimics a screening of  $\langle \mathbf{E}_{\text{dep}} \rangle$  via the  $\beta$  parameter. More precisely,  $\beta=0$  corresponds to ideal OC conditions, while an increase in  $\beta$  lowers the magnitude of the resulting depolarizing field, and  $\beta=1$  corresponds to ideal short-circuit (SC) conditions for which the depolarizing field has vanished. The third term of Eq. (2),  $E_{\text{surf}}$ , mimics how the existence of free surfaces affects the dipoles and strains near them.<sup>18,19</sup> Its analytical expression is indicated in Ref. 19, with its parameters having been determined from a first-principles computation on a PZT slab surrounded by vacuum. The total energy of Eq. (2) is used in Monte Carlo simulations,<sup>20</sup> with the ferroelectric dots being cooled down from high temperatures (in the paraelectric phase) to 10 K, in small steps.

Outputs of the simulations for our nanostructures include the local (magnetic or electric) dipole moments, which we generally denote as  $\{\mathbf{d}_i\}$  (i.e.,  $\mathbf{d}_i = \mu_i$  in the ferromagnetic ring and  $\mathbf{d}_i = \mathbf{p}_i$  in the ferroelectric dots). Such outputs allow us to compute the following quantities:

$$\begin{aligned} \mathbf{D} &= \frac{1}{Nv} \sum_i \mathbf{d}_i, \\ \mathbf{g} &= \frac{1}{2Nv} \sum_i \mathbf{r}_i \times \delta \mathbf{d}_i, \\ \mathbf{h} &= \frac{1}{4Nv} \sum_i \left[ \mathbf{r}_i \times (\mathbf{r}_i \times \delta \mathbf{d}_i) - \frac{1}{N} \sum_j \mathbf{r}_i \times (\mathbf{r}_j \times \delta \mathbf{d}_j) \right. \\ &\quad \left. - \frac{1}{N} \sum_j \mathbf{r}_j \times (\mathbf{r}_i \times \delta \mathbf{d}_j) \right], \end{aligned} \quad (3)$$

where the sums run over the cells of volume  $b^3$  in the ferromagnetic ring and over the primitive cells in the ferroelectric dots.  $N$  is the number of these cells,  $v$  is their volume, and  $\mathbf{r}_i$  locates their centers.  $\mathbf{D}$  is the polarization or magnetization, i.e., the typical order parameter of ferroelectrics or magnets.  $\delta \mathbf{d}_i$  is the difference between the dipole at cell  $i$  and the averaged (over all the cells) dipole, that is,  $\delta \mathbf{d}_i = \mathbf{d}_i - v\mathbf{D}$ . The quantity  $\mathbf{g}$  is the so-called toroidal moment, which has been recently defined and investigated from phenomenology<sup>9</sup> and first-principles-based computations.<sup>6,7,12,21–23</sup> On the other hand, we are not aware of any previous study mentioning the  $\mathbf{h}$  vector of Eq. (3). We decided to name it *the hypertoroidal moment*. It is important to realize that  $\mathbf{D}$ ,  $\mathbf{g}$ , and  $\mathbf{h}$  are all independent of the choice of the origin for the  $\{\mathbf{r}_i\}$  vectors in any zero-dimensional nanostructure, which makes them global rather than local quantities. One can convince oneself of this statement by analytically proving, from Eq. (3), that

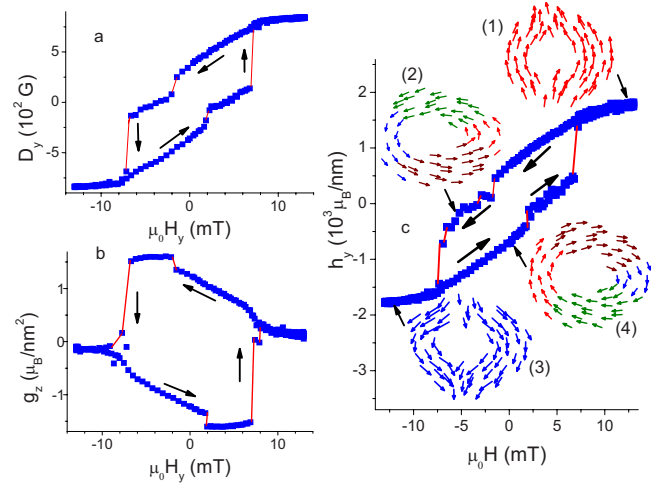


FIG. 1. (Color online) Predicted hysteresis loops in the studied asymmetric ferromagnetic ring. (a), (b), and (c) display the behavior of the magnetization, magnetic toroidal moment, and magnetic hypertoroidal moment, as functions of the applied homogeneous ac magnetic field. Insets schematize the dipole arrangement in the  $(x, y)$  plane for the states 1–4 (see text).

shifting all the  $\mathbf{r}_i$ 's by the same vector  $\mathbf{R}$  leaves  $\mathbf{D}$ ,  $\mathbf{g}$ , and  $\mathbf{h}$  unchanged. Such independency of  $\mathbf{R}$  partly originates from choosing  $\delta \mathbf{d}_i$  rather than  $\mathbf{d}_i$  in the definitions of  $\mathbf{g}$  and  $\mathbf{h}$ , and partly because  $\sum_i \delta \mathbf{d}_i = \mathbf{0}$ .

One aim of this paper is to undoubtedly prove that  $\mathbf{h}$  is an order parameter associated with the formation and evolution of some complex dipolar structures. For that, let us first focus on the investigated asymmetric ferromagnetic ring. Figures 1(a)–1(c) display its  $D_y$ ,  $g_z$ , and  $h_y$  as functions of  $\mu_0 H_y$ , respectively, at a simulated temperature of  $\approx 100$  K.  $\mu_0 H_y$  is the  $y$  component of the applied magnetic field, which is allowed to vary in time between  $-10$  and  $+10$  mT.  $D_y$  is the  $y$  (and sole) component of the magnetization of the nanoring,  $g_z$  is the  $z$  (and sole) component of the magnetic toroidal moment, and  $h_y$  is the  $y$  (and sole) component of the hypertoroidal moment. Figures 1 reveal that  $\mathbf{h}$  can be finite and can be considered as an order parameter, in addition to  $\mathbf{D}$  and  $\mathbf{g}$ , to represent the complex states, and their evolution, occurring in this ferromagnetic ring under a homogeneous magnetic field. More precisely, the insets in Fig. 1(c) provide a snapshot of the dipole arrangement in the four important states predicted by our simulations. These states are the following. State 1 is an ‘‘onion’’ state that occurs for the largest positive values of  $H_y$  and that does not possess any toroidal moment. This onion state rather exhibits the largest positive values for  $D_y$  and  $h_y$ . In fact, these two latter quantities are needed to fully characterize any onion state since  $D_y$  is the magnetization of the onion state while  $h_y$  provides a measure of the magnitude of the helicity of the two domains inherent in onion states (these two domains have semicircular magnetizations of opposite helicity<sup>24</sup>). State 2 is a vortex state characterized by a significantly positive  $g_z$  and vanishing  $D_y$  and  $h_y$ . State 3 is another onion state that differs from state 1 in the sign of its  $D_y$  and  $h_y$ . State 4 is a vortex state that differs from state 2 by adopting an opposite chirality (its  $g_z$  is now

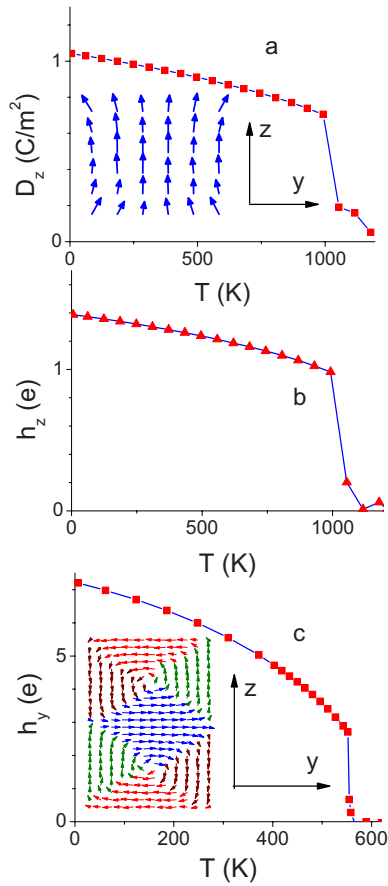


FIG. 2. (Color online) Temperature evolution of the polarization (a) and hyperferroic moment (b) in a stress-free cubic PZT dot of 24 Å lateral size and under ideal SC conditions, and of the hyperferroic moment (c) in a  $24 \times 48 \times 96$  Å<sup>3</sup> stress-free PZT dot under ideal OC conditions. Insets of (a) and (c) schematize the dipole arrangement for these two dots at 10 K. Temperature is scaled so that the theoretical Curie temperature for bulk  $\text{Pb}(\text{Zr}_{0.5}\text{Ti}_{0.5})\text{O}_3$  matches the experimental value.

negative). Our simulations further found that the pure onion states 1 and 3 “deform” themselves under the influence of the homogeneous magnetic field before transforming into the pure vortex states 2 and 4. This deformation mostly consists in pushing the wall between the two kinds of magnetized domains forming the onion state toward the thinner part of the asymmetric ring (i.e., toward the left side of the inner circle), as consistent with Refs. 5 and 25. This deformation leads to a decrease of the magnitude of  $D_y$  and  $h_y$  in favor of making  $g_z$  appear and increase in magnitude along the field path, as indicated by Figs. 1.

Let us now turn our attention to ferroelectric dots. The inset of Fig. 2(a) represents the dipole arrangement in the ground state of a stress-free cubic PZT dot of 24 Å lateral size, and under ideal SC conditions. As consistent with Ref. 7, this state is a flower state (note that flower states have also been seen in magnetic nanostructures of relatively small size<sup>26</sup>). It is polarized along the  $z$  direction but also exhibits a significant deviation, with respect to the  $z$  axis, for the direction of some local dipole moments. Such deviations, and their associated helical pattern, are typical of flower

states. As a result, any flower state should exhibit a nonzero polarization or magnetization, as well as a finite hyperferroic moment (which quantifies the helicity associated with such deviations), as numerically confirmed by Figs. 2(a) and 2(b), showing the evolution of  $D_z$  and  $h_z$  versus temperature, respectively, in our ferroelectric dot. These figures also reveal that the flower state forms around  $T_c \approx 1000$  K, and indicate that both  $D_z$  and  $h_z$  increase when the temperature is decreased below  $T_c$ —as a result of the increase of the magnitude of the local dipole moments.

An elongated  $24 \times 48 \times 96$  Å<sup>3</sup> stress-free PZT dot surrounded by vacuum all around it (that is, under ideal OC conditions) has also been investigated. The inset of Fig. 2(c) shows the resulting dipole pattern in its ground state. As consistent with Refs. 6 and 22, this pattern consists of two vortices having opposite chirality. This results in a vanishing toroidal moment, in addition to a null polarization. On the other hand, the hyperferroic moment of this state is found to be finite. In fact,  $\mathbf{h}$  can be considered as the sole order parameter of this “double” vortex, as confirmed by Fig. 2(c), which shows that the  $y$  component of  $\mathbf{h}$  is zero above a critical temperature  $T_h \approx 555$  K, and increases in magnitude when the temperature is decreased below  $T_h$ . (The two other Cartesian components of  $\mathbf{h}$  are null for any temperature.) Such features indicate that the double vortex forms at  $T_h$  with the centers of these two vortices being aligned along the  $z$  axis [as seen in the inset of Fig. 2(c)], and that the dipoles inside these two opposite vortices grow larger in magnitude as the temperature is reduced below  $T_h$ .

Other phases are associated with a hyperferroic moment. One example is the so-called antiferroferroic state that was recently predicted in arrays of ferroelectric nanodots embedded into a polarizable media, and that consists of periodically alternating vortices of opposite chirality.<sup>8</sup> Other examples are the recently discovered out-of-plane 180° nanostripe domains,<sup>2</sup> as well as the predicted ferroelectric bubbles,<sup>4</sup> in ferroelectric thin films: we numerically found that these complex states possess a finite  $\mathbf{h}$ . (Note, however, that the magnitude of  $\mathbf{h}$ , and even its sign, depend in practice on the periodic supercell one uses to mimic thin films.) Such a nonzero hyperferroic moment should also occur in their magnetic counterparts, namely, for magnetic stripes and magnetic bubbles in ferromagnetic films.<sup>1</sup>

In summary, we used computational schemes to discover an order parameter that characterizes the formation and evolution of many complex dipolar structures. This parameter is denoted the hyperferroic moment and involves the second moment of the local dipole moments, unlike the polarization or magnetization and toroidal moment, which are associated with their zeroth and first moments, respectively. One may also wonder if the order parameters defined in Eq. (3) are enough to characterize any known complex dipolar structure. Interestingly, this is not the case, since we found that the “antivortex” state or “hedgehog topological” defects<sup>27</sup> need rather to be described by a finite  $Q^{(d)}$  and finite  $q_{\alpha\gamma}^{(d)}$  where  $Q^{(d)} = (1/3Nv) \sum_i \mathbf{r}_i \cdot \delta \mathbf{d}_i$  and  $q_{\alpha\gamma}^{(d)} = (1/2Nv) \sum_i (r_{i\alpha} \delta d_{i\gamma} + r_{i\gamma} \delta d_{i\alpha}) - \delta_{\alpha\gamma} Q^{(d)}$  (with  $\alpha$  and  $\gamma$  being Cartesian components). Such findings imply that one should, in fact, consider many moments of the local dipole moments to fully repre-

sent any known, or even remaining-to-be-discovered, dipolar state. Finally, let us note that the hypertoroidal moment may lead to the design of devices with efficient and/original functionalities, if one succeeds in controlling its magnitude and direction.

We thank Inna Ponomareva for useful discussions and providing us with some codes. This work was mostly sup-

ported by DOE Grant No. DE-FG02-05ER46188. We also acknowledge support from ONR Grant No. N00014-04-1-0413 and NSF Grants No. DMR-0701558, No. DMR-0404335, and No. DMR-0080054 (C-SPIN). Some computations were made possible thanks to the MRI Grants No. 0421099 and No. 0722625 from NSF. S.P. also appreciates RFBR Grants No. 07-02-00099 and No. 05-02-90568NNS.

- 
- <sup>1</sup>A. Hubert and R. Schafer, *Magnetic Domains: The Analysis of Magnetic Microstructures* (Springer, Berlin, 1998).
- <sup>2</sup>S. K. Streiffer, J. A. Eastman, D. D. Fong, C. Thompson, A. Munkholm, M. V. Ramana Murty, O. Auciello, G. R. Bai, and G. B. Stephenson, *Phys. Rev. Lett.* **89**, 067601 (2002).
- <sup>3</sup>I. Kornev, H. Fu, and L. Bellaiche, *Phys. Rev. Lett.* **93**, 196104 (2004).
- <sup>4</sup>B.-K. Lai, I. Ponomareva, I. I. Naumov, I. Kornev, Huaxiang Fu, L. Bellaiche, and G. J. Salamo, *Phys. Rev. Lett.* **96**, 137602 (2006).
- <sup>5</sup>C. L. Chien, F. Q. Zhu, and J.-G. Zhu, *Phys. Today* **60**(6), 40 (2007).
- <sup>6</sup>I. Naumov, L. Bellaiche, and H. Fu, *Nature (London)* **432**, 737 (2004).
- <sup>7</sup>I. Ponomareva, I. I. Naumov, I. Kornev, Huaxiang Fu, and L. Bellaiche, *Phys. Rev. B* **72**, 140102(R) (2005); I. Ponomareva, I. I. Naumov, and L. Bellaiche, *ibid.* **72**, 214118 (2005).
- <sup>8</sup>S. Prosandeev and L. Bellaiche, *Phys. Rev. Lett.* **97**, 167601 (2006).
- <sup>9</sup>V. M. Dubovik and V. V. Tugushev, *Phys. Rep.* **187**, 145 (1990).
- <sup>10</sup>V. M. Dubovik, M. A. Martsenyuk, and B. Saha, *Phys. Rev. E* **61**, 7087 (2000).
- <sup>11</sup>H. Hoffmann and F. Steinbauer, *J. Appl. Phys.* **92**, 5463 (2002).
- <sup>12</sup>S. Prosandeev, I. Ponomareva, I. Kornev, and L. Bellaiche, *Phys. Rev. Lett.* **100**, 047201 (2008).
- <sup>13</sup>M. E. Schabes and H. N. Bertram, *J. Appl. Phys.* **64**, 1347 (1988).
- <sup>14</sup>V. P. Antropov, S. V. Tretyakov, and B. N. Harmon, *J. Appl. Phys.* **81**, 3961 (1997).
- <sup>15</sup>W. Zhong, D. Vanderbilt, and K. M. Rabe, *Phys. Rev. Lett.* **73**, 1861 (1994).
- <sup>16</sup>L. Bellaiche, A. García, and D. Vanderbilt, *Phys. Rev. Lett.* **84**, 5427 (2000).
- <sup>17</sup>I. I. Naumov and H. Fu, arXiv:cond-mat/0505497 (unpublished).
- <sup>18</sup>H. Fu and L. Bellaiche, *Phys. Rev. Lett.* **91**, 257601 (2003).
- <sup>19</sup>E. Almahmoud, Y. Navtsenya, I. Kornev, H. Fu, and L. Bellaiche, *Phys. Rev. B* **70**, 220102(R) (2004).
- <sup>20</sup>N. Metropolis, A. W. Rosenbluth, M. N. Rosenbluth, A. H. Teller, and E. Teller, *J. Chem. Phys.* **21**, 1087 (1953).
- <sup>21</sup>S. Prosandeev, I. Ponomareva, I. Kornev, I. Naumov, and L. Bellaiche, *Phys. Rev. Lett.* **96**, 237601 (2006).
- <sup>22</sup>S. Prosandeev and L. Bellaiche, *Phys. Rev. B* **75**, 094102 (2007).
- <sup>23</sup>S. Prosandeev, I. Kornev, and L. Bellaiche, *Phys. Rev. B* **76**, 012101 (2007).
- <sup>24</sup>J. Rothman, M. Kläui, L. Lopez-Diaz, C. A. F. Vaz, A. Bleloch, J. A. C. Bland, Z. Cui, and R. Speaks, *Phys. Rev. Lett.* **86**, 1098 (2001).
- <sup>25</sup>F. Q. Zhu, G. W. Chern, O. Tchernyshyov, X. C. Zhu, J. G. Zhu, and C. L. Chien, *Phys. Rev. Lett.* **96**, 027205 (2006).
- <sup>26</sup>M. E. Schabes and H. N. Bertram, *J. Appl. Phys.* **64**, 1347 (1988).
- <sup>27</sup>P. M. Chaikin and T. C. Lubensky, *Principles of Condensed Matter Physics* (Cambridge University Press, Cambridge, U.K., 2000).